

Laboratory Tests of a Residential Low-Temperature Water Source Heat Pump

V.C. Mei, Ph.D., P.E.
ASHRAE Member

ABSTRACT

A residential unitary low-temperature water-source heat pump was tested in the laboratory. Tests were performed over a broad range of source-water temperature 45 to 70°F (7.2 to 21.1°C) and water-flow rates 5 to 30 gpm ($3.2 \times 10^{-4} \text{ m}^3/\text{s}$ to $8.2 \times 10^{-4} \text{ m}^3/\text{s}$).

The heat pump capacity and coefficient of performance (COP) were found to be linearly related to the source-water temperatures. In the heating mode, the capacity and COP increased with increasing source-water temperature and flow rate. In the cooling mode, the capacity and COP decreased with increasing source-water temperature but increased with increasing water-flow rate. However, when an assumed water-pumping power, for a 150 ft (46 m) total head, was taken into account in the COP calculation, it was found that the net COP for both heating and cooling decreased with increasing water-flow rate.

For cyclic operation over the tested source-water temperature range, the coefficient of degradation, C_D , ranged from 0.196 to 0.137 for heating and from 0.131 to 0.161 for cooling. The effect of inlet air humidity was also studied for cooling mode operation.

A sample calculation is included in the paper to demonstrate the application of the test results in calculating the annual performance factor (APF). The test results are used to form a data base on the performance of a typical residential, unitary low-temperature water-source heat pump.

INTRODUCTION

Groundwater temperature in the continental United States ranges from a low of about 42°F (5.6°C) in the northernmost regions to a high of about 78°F (25.6°C) in the Deep South. This water provides an ideal heat source or sink for year-round heating and cooling with water-source heat pumps. Since the groundwater temperature stays almost constant year round, regardless of the extremes of the ambient air temperature, a properly designed groundwater heat pump system will operate at a higher seasonal performance factor than an air-to-air unit in the same climate. However, the expensive well drilling limited such systems to those areas where abundant high-temperature groundwater was available at moderate depths.

Ever escalating energy costs in recent years have brought about a search for more energy-efficient residential space conditioning. It is apparent that groundwater heat pumps can provide significant energy savings, and the old idea of using a groundwater-coupled heat pump has become a promising prospect for energy conservation. Many water-source heat pumps are now designed to operate on relatively cold groundwater, as low as 40°F (4.4°C), which extends considerably their geographic range of applicability. Although the low-temperature groundwater heat pumps are becoming more popular,

well-instrumented test data are still quantitatively inadequate. The purpose of this study was to collect sufficient information to form an initial data base on the performance of a typical residential, unitary low-temperature water-source heat pump.

The experiment described in this report can be divided into four parts, steady-state and cyclic operations for both heating and cooling modes. For steady-state operation, the tests were performed with inlet water temperature and water-flow rate as parameters. In addition, the effect of inlet air moisture content on the heat pump performance was also tested for cooling-mode operation.

For cycling tests, the cycling loss, which is caused by refrigerant migration from the high- to the low-pressure side during the off-cycle, was experimentally determined with inlet water temperature and water-flow rate as parameters. For cooling-mode cycling tests, both dry-coil and wet-coil tests were performed under the same operating conditions to confirm that cycling loss is independent of the level of inlet air humidity, as concluded by Didion and Kelly (1979).

In order to estimate the annual performance factor, APF, the degradation coefficient was calculated with inlet water temperature and flow rates as the parameters. Finally, an example of estimating the APF for a known house load is presented to demonstrate the application of the test data.

DESCRIPTION OF TEST UNIT

The heat pump tested is of commercially available unitary design with an air-handling compartment above another compartment containing the compressor and the water-to-refrigerant heat exchanger. The two compartments are separated by an insulated panel. The manufacturer's rated heating and cooling capacities for the unit are 42,100 Btu/h (12.34 kW) and 33,500 Btu/h (9.82 kW), respectively, for 65°F (18.3°C) water at 11 gpm ($6.9 \times 10^{-4} \text{ m}^3/\text{s}$).

The compressor had a nominal rating of 2 1/2 hp and R-22 was the refrigerant. The blower of the air-handling system, with a three-speed, 1/2 hp motor, was rated at 1,500 cfm ($7.1 \times 10^{-4} \text{ m}^3/\text{s}$) at 0.1 in water (24.7 Pa) external pressure.

Refrigerant flow in both heating and cooling modes was controlled by a single thermal expansion valve, with the temperature-sensing bulb on the compressor suction line. The refrigerant charge recommended by the manufacturer was 3.50 lb (1.59 kg). However, extra copper tubing was added to the system for installation of the instruments, which increased the total volume of the refrigerant circuit, and additional 3.60 lb (1.63 kg) of R-22 was added to the system.

The water-to-refrigerant heat exchanger is of coaxial tube in tube design, with a helical screw-threaded inner tube to enhance the flow turbulence and heat-transfer area. Refrigerant flows in the annulus area and water in the inner tube. An external water-circulation pump was installed to circulate the water through the heat exchanger.

DESCRIPTION OF TEST APPARATUS

The test apparatus was built to measure both air-side and refrigerant-side energy changes across the air-to-refrigerant heat exchanger, water and refrigerant energy changes across the water-to-refrigerant heat exchanger, and power consumption of the compressor and blower motors. Figure 1 shows the refrigerant and water circulating loops and the location of pressure and temperature sensors and flow-rate measuring devices.

A "bootstrap" loop was built around the heat pump air-handling compartment to provide some control over the inlet air temperature with the recirculation of part of the heat pump exit air.

Airflow rate was determined by a duct air-monitoring device with 1 ft² (0.092 m²) cross-sectional area; it measures the average velocity head of the inlet air. A low-pressure differential transducer converted the velocity head into DC voltage as input signal to the data acquisition system for air-velocity calculation. Average air temperatures entering and leaving the unit were measured by sets of nine thermocouples connected in parallel. Two humidity sensors were used to measure the air relative

humidities for heating-mode tests. For cooling-mode tests, wet-bulb temperatures of entering and leaving air were measured by two single thermocouples covered with wetted wicks.

The refrigerant flow rate was measured by a turbine flowmeter connected in series with a rotameter that also served as a sight glass. The refrigerant pressure drops across the air-to-refrigerant and the water-to-refrigerant heat exchangers were measured by four pressure transducers. The refrigerant temperatures at various locations, as shown in figure 1, were measured by single thermocouples clamped on the refrigerant lines and covered with insulation. Pressure gauges were installed to visually check the pressures on the compressor suction and discharge lines, as well as the pressures before and after the expansion valve.

The water flow rate was measured by a turbine flowmeter connected in series with a rotameter. The inlet and outlet water temperatures were measured by single thermocouples in wells installed at the inlet and outlet water line fittings.

A 1,000 gal (3.8 m³) water tank was used as the water supply tank, and an icemaker on top of the tank could chill the water down to 32°F (0°C).

The heat pump compressor power and blower power consumption were measured by two thermal-watt converters.

A steam line was installed near the air intake duct to boost the intake air humidity when the intake air was dry. A small steam coil was installed in the intake air ductwork, which could raise the inlet air temperature by 2.5°F (1.4°C) to provide the fine adjustment of the intake air temperature.

TEST PROCEDURE

Tests were conducted to study the response of performance parameters to changes of water temperature and water-flow rate while the heat pump was in operation. The tests were run at water temperatures ranging from 45 to 70°F (7.2 to 21.1°C) and water-flow rates of 5 to 13 gpm (3.2×10^{-4} to 8.3×10^{-4} m³/s).

Since most heat pumps are rated without concern for the water-pumping power consumption, a calculated pumping power was added in order to estimate the system performance. A 150 ft (45.7 m) total water head and a pump efficiency of 0.3 are assumed. The pumping power can then be calculated by the following equation:

$$P_{\text{pump power}} = 0.415 \cdot \dot{m}_w \quad (1)$$

where

\dot{m}_w is the water mass flow rate in kg/h and the pump power is in W.

Steady-State Tests

The water in the storage tank was first heated to 80°F (26.7°C) for the heating mode or chilled down to 35°F (1.7°C) for cooling-mode operation. The heat pump was then operated with water from the storage tank at a selected water-flow rate. The water went through the water-to-refrigerant heat exchanger and was recirculated back to the storage tank, which caused the tank water temperature to decrease (heating mode) or increase (cooling mode) slowly at a rate of about 7 to 10 min/°F (12.5 to 18 min/°C). Since the water temperature in the tank changed slowly, it was reasonable to assume that the heat pump was tested under quasi-steady state while the test data were collected. The data collection started when the water temperature reached 70°C (21.1°C) for the heating mode or 45°F (7.2°C) for the cooling mode and continued until the range of the water temperatures set for the test was satisfied.

For cooling-mode steady-state tests with inlet air humidity as the parameter, tap water was used because of its constant temperature. The heat pump was in operation for at least one hour before the data collection started. Steam was injected into the heat pump inlet air while the air dry-bulb temperature was held constant at $80 \pm 0.5^\circ\text{F}$ ($26.7 \pm 0.3^\circ\text{C}$). The tests were conducted at water-flow rates

of 5 and 9 gpm (3.2×10^{-6} and 5.8×10^{-4} m³/s) with inlet wet-bulb varying from 55 to 70°F (12.8 to 21.1°C) and with water inlet temperature at 54°F (12.2°C).

Cycling Tests

The cycling tests were performed on a 6-minutes-on and 24-minutes-off time schedule for the same water-flow rates and water-temperature ranges as those for steady-state tests.

The water temperature in the storage tank was first adjusted to 10°F (5.6°C) above (heating mode) or below (cooling mode) the selected water temperature set for the test. The water was recirculated back to the tank while the heat pump was in operation. By the time the water temperature in the tank decreased (or increased) to the set temperature, the heat pump would have already been operated for more than an hour and would be in quasi-steady state condition. The heat pump was then shut off for a period of 24 minutes to start the cycling test. During the six-minutes-on period, the water from the tank that went through the heat exchanger was drained to the sink so that a constant water temperature in the storage tank could be maintained. A minimum of four on/off cycles were performed for each test.

For cooling-mode cyclic operation, two tests were performed under wet-coil conditions at 37% and 50% relative humidity.

TEST RESULTS OF STEADY STATE OPERATION

Heating Mode

Figure 2 shows the capacity as a function of water temperature with the water-flow rate as a parameter. It shows that the capacity increases with increasing water-flow rate. At 55°F (12.8°C) inlet water temperature, the capacity increases from 35,000 Btu/h (10.3 kW) at 5 gpm (3.2×10^{-4} m³/s) to 38,000 Btu/h (11.2 kW) at 13 gpm (8.3×10^{-4} m³/s). The capacity increase is very small compared with the percentage increase of water-flow rate.

Figure 3 shows the COP as a function of entering water temperatures with water-flow rate as the parameter. The solid lines are those COPs calculated without including the water-pumping power. It can be seen that the higher the water-flow rate, the higher the COP. The dashed lines are the COPs calculated with an assumed water-pumping power, as mentioned before. The dashed lines indicate that the higher the water-flow rate, the lower the COP. It is clear that the heat pump is to be operated at higher overall COP, it must be operated at a lower water-flow rate with a slightly reduced heating capacity.

Cooling Mode

Figure 4 shows the heat pump total and sensible capacities as functions of inlet air wet-bulb temperature. The figure indicates that the total capacity increases when the inlet air becomes more humid, but the sensible capacity decreases. The effect of inlet air humidity on the capacities is clearly exponential.

Figure 5 shows the total and sensible capacities as functions of inlet water temperature with water-flow rate as the parameter. It is seen that the water-flow rate has little effect on either capacity. For example, at 55°F (12.8°C) water temperature, the total capacity increases from 33,100 to 34,800 Btu/h (9.7 to 10.2 kW) a 5% increase, while the water-flow rate increases from 5 to 13 gpm (3.2×10^{-4} to 8.7×10^{-4} m³/s), a 260% increase. The example indicates that the heat pump cooling-capacity output is not very sensitive to the water-flow rate.

Figure 6 shows the COP as a function of inlet water temperature with water-flow rate as the parameter. Again, when the assumed water pumping-power is included in the COP calculation, the higher the water flow rate, the lower the COP. The water pump power input makes the low water-flow rate operation preferable.

TEST RESULTS OF CYCLIC OPERATION

Figure 7 shows a typical heating-mode cycling test at 7 gpm ($4.5 \times 10^{-4} \text{ m}^3/\text{s}$) and 50°F (10°C) inlet water temperature. The power peaks at the start of the on-cycle. The capacity output increases sharply for the first 60 seconds of operation and then approaches the steady state capacity asymptotically. A great portion of the cycling loss happens at the first minute of operation, when the capacity output is small and the power consumption is high.

Figure 8 shows the cycling loss as a function of water inlet temperature with water-flow rate as the parameter. It indicates that the cycling loss is independent of water-flow rate. The loss decreases linearly with the increasing water temperature for the heating mode and decreasing water temperature for cooling-mode operation. The loss ranges from 11.3% at 70°F (21.1°C) to 16.5% at 45°F (7.2°C) for heating and from 10.8% at 45°F (7.2°C) to 13.5% at 70°F (21.1°C) for cooling.

Figure 9 shows the cooling-mode cycling loss as a function of inlet air relative humidity. The tests performed at 37% and 50% relative humidity were wet-coil operations, where moisture condensation had occurred during the six-minutes-on cycle. The two tests with relative humidity less than 30% were dry-coil operations. It can be seen that the cooling mode cycling loss is independent of the inlet air moisture content as stated by Didion and Kelly (1979).

Figure 10 shows the degradation coefficient, C_D , as a function of water inlet temperature. The calculation of C_D (Didion and Kelly 1979), based on the cycling loss and load factor, enables one to estimate the heat pump annual performance factor, APF. It can be seen that C_D can be expressed as a linear function of water temperature only. The values of C_D vary from 0.2 to 0.14 for the heating mode and 0.13 to 0.16 for the cooling mode over the range of water temperatures from 45 to 70°F (7.2 to 21.1°C).

A SAMPLE CALCULATION OF WATER SOURCE HEAT PUMP ANNUAL PERFORMANCE FACTORS

The sample calculation was based on an assumed $1,800 \text{ ft}^2$ (167 m^2) house located in Nashville, TN, with $40.9 \times 10^6 \text{ Btu}$ (0.0120 mkwh) annual heating load and $31.4 \times 10^6 \text{ Btu}$ (0.0092 mkwh) cooling load, respectively. The groundwater temperature was assumed to be 57°F (13.9°C). Since the tested heat pump capacity output was too high for the house, the capacity and power input were scaled down to $2\frac{1}{2}$ tons (8.8 kW) of designed cooling capacity, which was about 10% oversized. In order to calculate the power input to the water pump, the water head (which included the depth to water level), the water pressure drop across the water-to-refrigerant heat exchanger, and the frictional loss were assumed to be 100, 150, and 200 ft (30.5, 45.6, and 61.9 m) respectively, along with an assumed pump-motor efficiency of 0.3.

The following steps were taken to calculate the heat pump annual performance factor, APF.

1. The house load, \dot{Q}_{load} , was calculated by the monthly temperature bin method with the computer program MAD (Ballou, Nephew, and Abbatiello 1981).
2. From the results of the heat pump steady-state tests were found the steady state capacity output, \dot{Q}_{ss} , and $(\text{COP})_{ss}$.
3. The load factor was calculated by dividing the house load, \dot{Q}_{load} , with heat pump steady-state load.

$$L_F = \frac{\dot{Q}_{load}}{\dot{Q}_{ss}} \quad (2)$$

4. With the known degradation coefficient, C_D , the $(\text{COP})_{cyc}$ could be calculated with the following equation.

$$C_D = \frac{1 - \frac{(\text{COP})_{cyc}}{(\text{COP})_{ss}}}{1 - L_F} \quad (3)$$

5. Since \dot{Q}_{load} and $(COP)_{cyc}$ were calculated, the power input to the heat-pump cyclic operation could be estimated by dividing \dot{Q}_{load} with $(COP)_{cyc}$.
6. The heat-pump annual performance factors could be calculated by summarizing the house load, both heating and cooling, and then dividing it by the total power input into the system, which included the power input to the compressor motor, fan motor, and water pump motor.

The degradation coefficient, C_D , was 0.168 for the heating mode and 0.147 for the cooling mode, as determined by the test for a source-water temperature of 55°F (13.9°C).

Table 1 shows the heat-pump heating and cooling capacities and COP as functions of water-flow rate but without water-pumping power. Capacity and COP scaling down factors used are also shown in the table. Table 2 shows the water-pump power consumption as a function of water-flow rate and pump head. Table 3 shows the APF as a function of water-flow rate/ton cooling and total pump head with cycling loss. In all cases, it can be seen that lower head has higher APF. Table 4 is the same as table 3, except cycling loss is not included, by assuming $C_D = 0$ for both heating and cooling. If one compares the APF shown in tables 3 and 4, it can be seen that the heat pump APFs increase about 10% if cycling loss can be eliminated. The data listed in tables 3 and 4 are shown graphically in figure 11. It is clear that APF is strongly affected by the total head.

DISCUSSION AND CONCLUSION

For both heating and cooling, the capacity and COP of the heat pump under test could both be considered linear functions of inlet water temperature over the range from 45 to 70°F (7.2 to 21.1°C).

The steady-state heating capacity and COP increased with increasing inlet water temperature and water-flow rate if the water circulating pump power was not considered. The steady state cooling capacity and COP decreased with increasing entering water temperature and increased with increasing water-flow rate, although the effect of the water flow rate on the capacity and COP was very small.

For both heating and cooling steady-state COP calculation, if the water pump power input is included and a total head of 150 ft (46 m) and a pump-motor efficiency of 0.3 are assumed, the COP decreased with increasing water-flow rate.

For cooling-mode steady-state operation, an increase of inlet air humidity increased the heat-pump total capacity but decreased the sensible capacity output.

Both heating- and cooling-mode cycling tests were performed on a 6-minutes-on/24-minutes-off time schedule. For heating-mode cyclic operation, the cycling loss decreased with an increase in entering water temperature from 45 to 70°F (7.2 to 21.1°C). The degradation coefficient was from 0.196 to 0.147 over the same water temperature range. For cooling-mode cyclic operation, both dry-coil and wet-coil tests were performed at a constant water-flow rate and entering temperature. The results indicated that the cycling loss was independent of the humidity of the entering air. The cycling loss, which increased with increasing water temperature, ranged from 10.7% to 13.4% over the entering water temperature range, 45 to 70°F (7.2 to 21.1°C). The degradation coefficient ranged from 0.132 to 0.161 over the same water temperature range.

The cycling loss and degradation coefficient, for both heating- and cooling-mode operation, were independent of water-flow rate.

The effect of extra refrigerant added to the system on the heat pump performance cannot be checked easily. For steady-state operation, the test data were compared with the manufacturer's published information and found to be very close. It is, therefore, reasonable to assume that the effect of extra refrigerant charging is negligible. However, such comparison for cyclic operation cannot be made due to inadequate test data. It is an interesting subject for future studies.

NOMENCLATURE

APF	=	Annual performance factor
C_D	=	Degradation coefficient
$(COP)_{cyc}$	=	Coefficient of performance under cyclic operation
$(COP)_{ss}$	=	Coefficient of performance under steady-state operation
L_F	=	Load factor
\dot{m}	=	Water-flow rate
$P_{\text{pump power}}$	=	Water circulating pump power consumption
Q_{load}	=	House load
Q_{ss}	=	Heat pump steady-state capacity

REFERENCES

Didion, D.A., and Kelly, G.E. 1979. "New testing and rating procedures for seasonal performance of heat pump." ASHRAE J., Sept.

Ballou, M.L.; Nephew, E.A.; and Abbatiello, L.A. 1981. "MAD: A Computer program for ACES design using monthly thermal loads." ORNL/CON-51, 3-1981.

ACKNOWLEDGMENTS

This research was sponsored by the Office of Buildings Equipment Research and Development, U.S. Department of Energy, under contract W-7405-eng-26 with the Union Carbide Corporation.

TABLE 1
Steady-State Water-Source Performance Data^a

Water-Flow Rate		Heating Mode			Cooling Mode			2½ Ton
gpm	(m ³ /s)	Capacity		COP ^b	Capacity		EER ^b	Scaling Factor
		KBtu/h	(kW)		KBtu/h	(kW)		
3.0	(1.9 × 10 ⁻⁴) ^c	34.7	(10.2)	3.12	30.5	(8.9)	9.39	0.987
5.0	(3.2 × 10 ⁻⁴)	35.9	(10.5)	3.15	32.5	(9.5)	10.51	0.926
9.0	(5.8 × 10 ⁻⁴)	37.8	(11.1)	3.22	34.5	(10.1)	11.47	0.872
13.0	(8.7 × 10 ⁻⁴)	39.2	(11.5)	3.30	34.7	(10.2)	11.88	0.867

^aHeat pump entering water temperature was 57°F (13.9°C)

C_D (Degradation Coefficient) = 0.168 for heating

C_D = 0.147 for cooling

^bCOP and EER were calculated without including water pump power input.

^cThe data on this water-flow rate were extrapolated.

TABLE 2
Assumed Water Pump Power Input^a

Water-Flow Rate		Assumed Total Head, ft(m)		
gpm	(m ³ /s)	100.0 (30.5)	150.0 (45.7)	200.0 (61)
Water Pump Power Input, W				
3.0	(1.9 × 10 ⁻⁴)	188	282	376
5.0	(3.2 × 10 ⁻⁴)	314	471	628
9.0	(5.8 × 10 ⁻⁴)	565	848	1130
13.0	(8.7 × 10 ⁻⁴)	817	1225	1634

^aPump power input calculation was under the assumption of pump efficiency equal to 0.3 (see detailed pump power input calculation).

TABLE 3
Water Source Heat Pump Annual Performance Factor^a

Water-Flow Rate/ton cooling		Total Pump Head			<i>C_D</i>	<i>C_D</i>
gpm/tons	(m ³ /s Ton _c)	ft (m)			Cooling	Heating
		100.0 (30.5)	150.0 (45.7)	200.0 (61.0)		
Annual Performance Factor						
1.18	(0.75 × 10 ⁻⁴)	2.54	2.47	2.40	0.168	0.147
1.85	(1.2 × 10 ⁻⁴)	2.59	2.46	2.37		
3.13	(2.0 × 10 ⁻⁴)	2.54	2.36	2.21		
4.50	(3.0 × 10 ⁻⁴)	2.44	2.22	2.03		

^awith cycling loss

TABLE 4
Water Source Heat Pump Annual Performance Factor^b

Water-Flow Rate/Ton _{cooling}		Total Pump Head			<i>C_D</i>	<i>C_D</i>
gpm/ton _c	(Liter/s Ton _c)	ft(m)			Heating	Cooling
		100.0 (30.5)	150.0 (45.7)	200.0 (61.0)		
Annual Performance Factor						
1.18	(0.075)	2.78	2.71	2.64	0	0
1.85	(0.12)	2.84	2.72	2.60		
3.13	(0.20)	2.79	2.59	2.42		
4.50	(0.30)	2.68	2.43	2.23		

^bwith no cycling loss

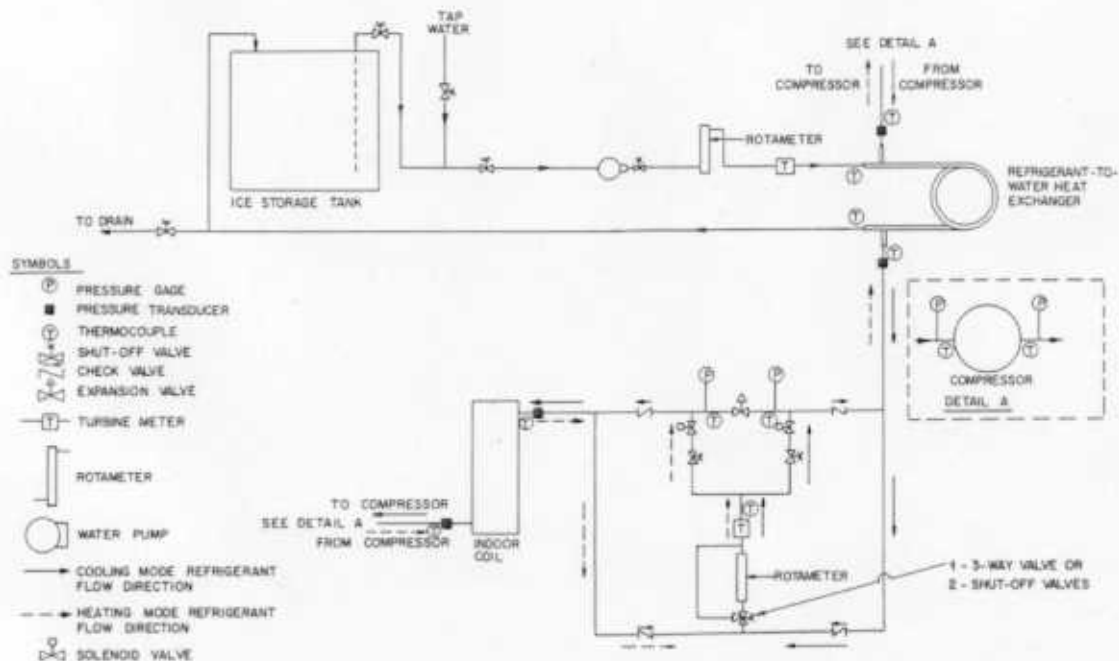


Figure 1. Schematic of refrigerant and water loops

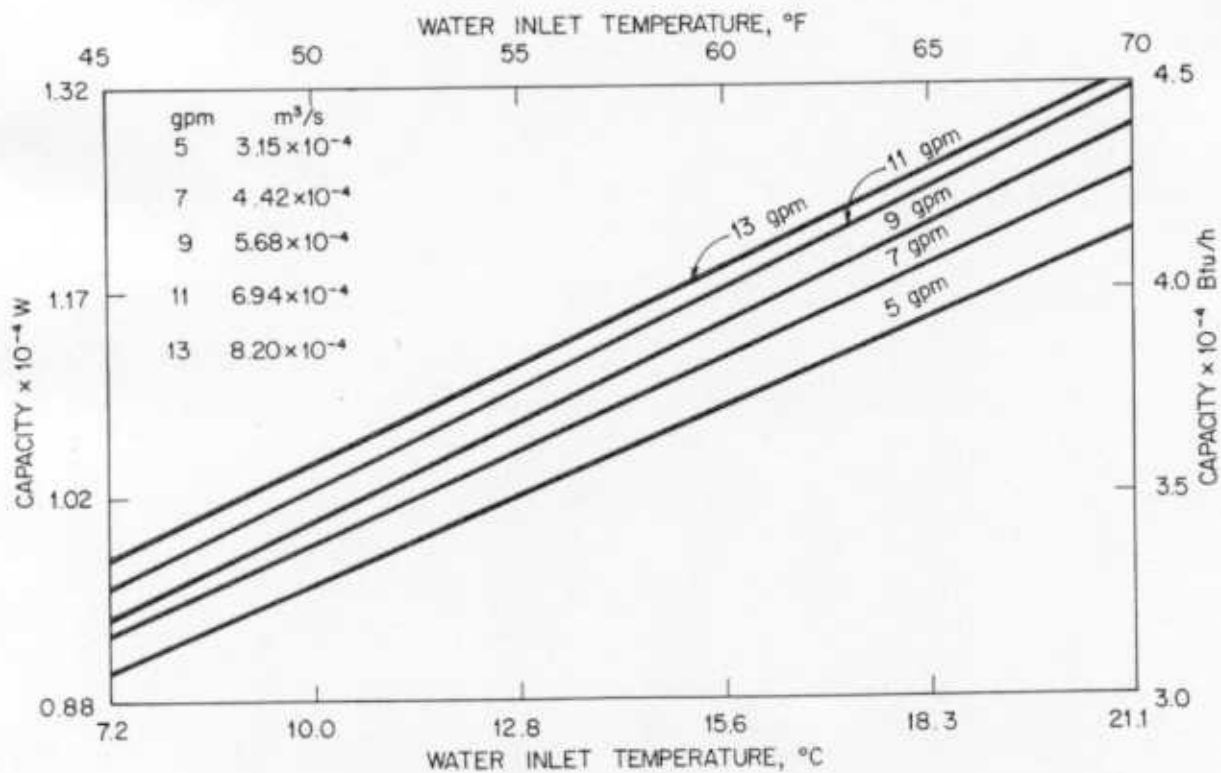


Figure 2. Steady-state heating capacity versus water inlet temperature

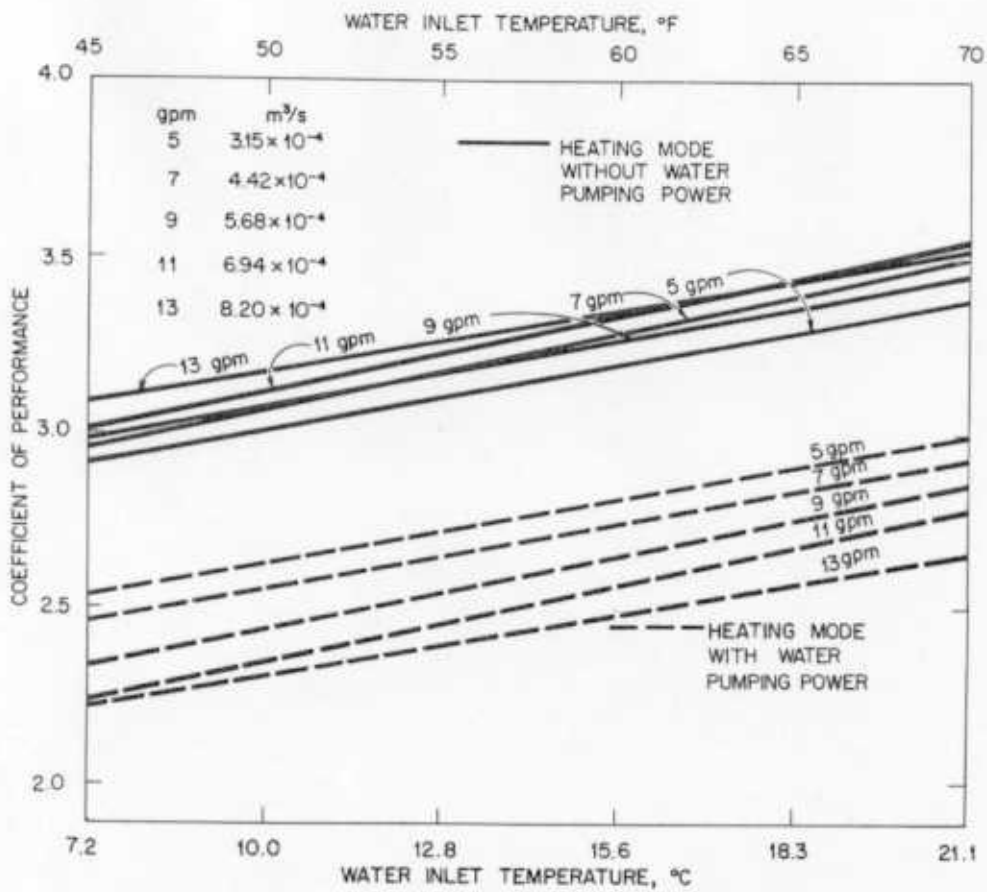


Figure 3. Steady-state heating COP versus water inlet temperature

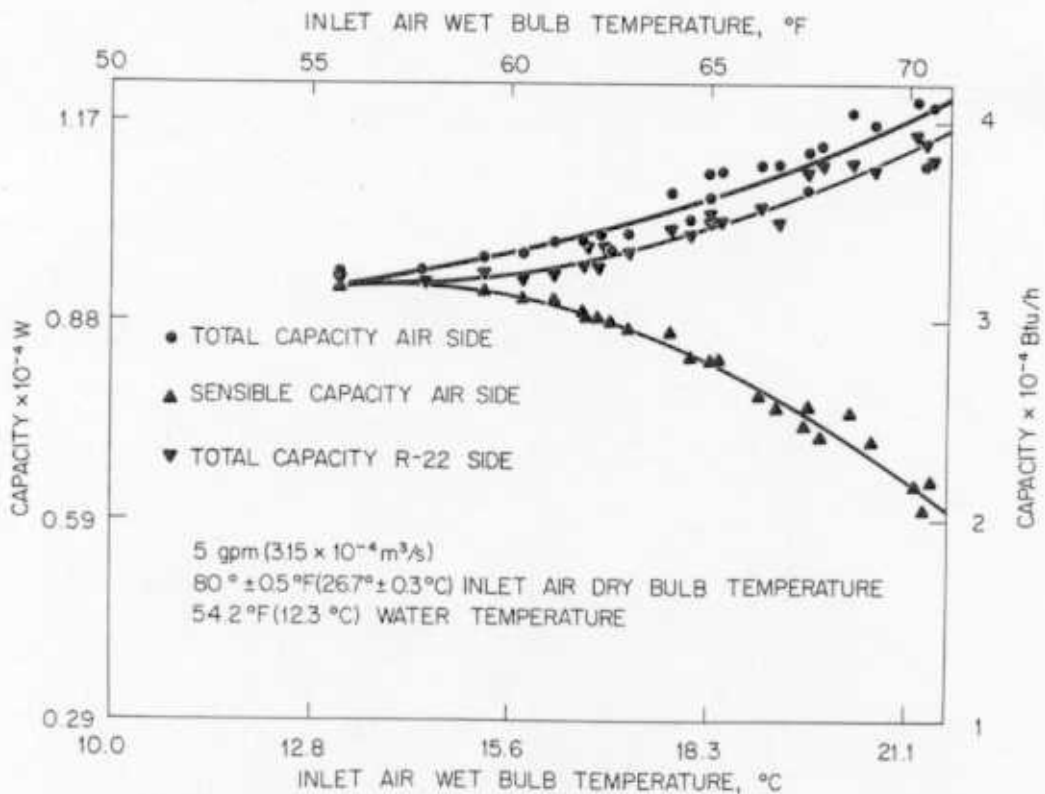


Figure 4. Steady-state cooling capacity versus inlet air wet bulb temperature

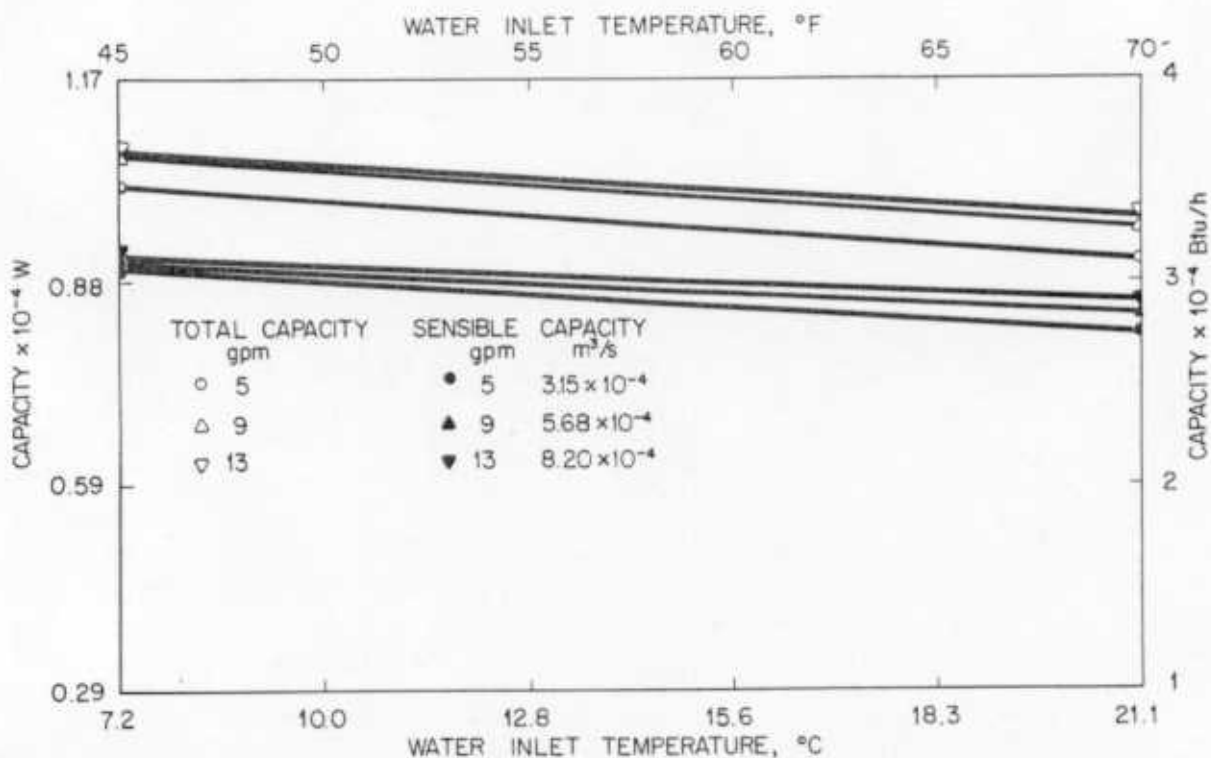


Figure 5. Steady-state cooling capacity versus water inlet temperature

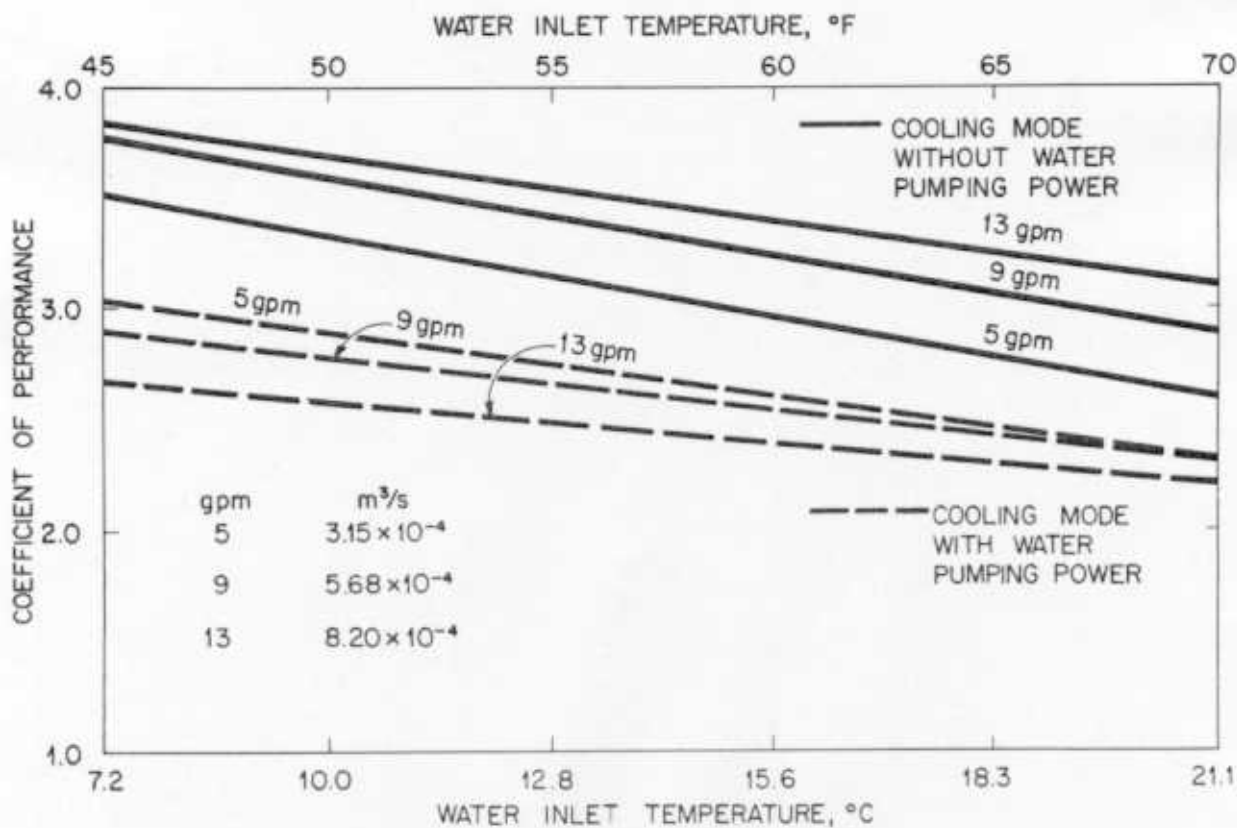


Figure 6. Steady-state cooling COP versus water inlet temperature

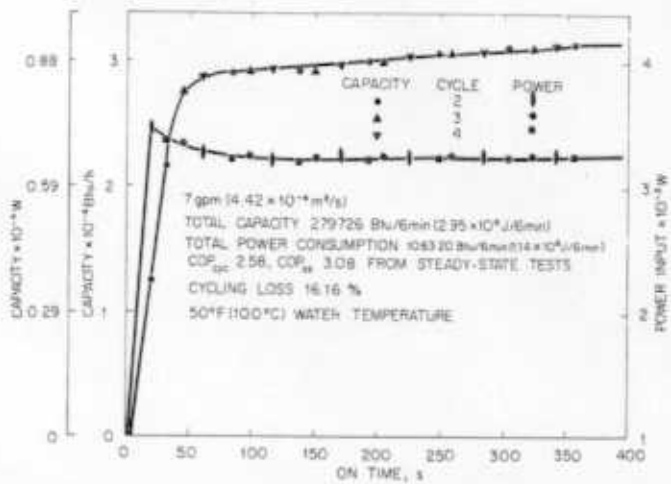


Figure 7. A typical heating cycling test

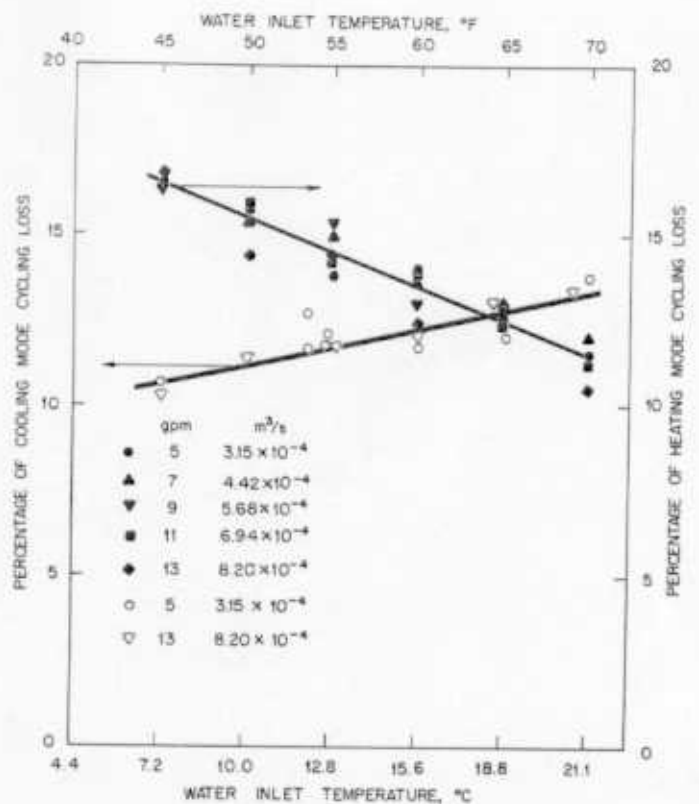


Figure 8. Cycling losses versus water inlet temperature

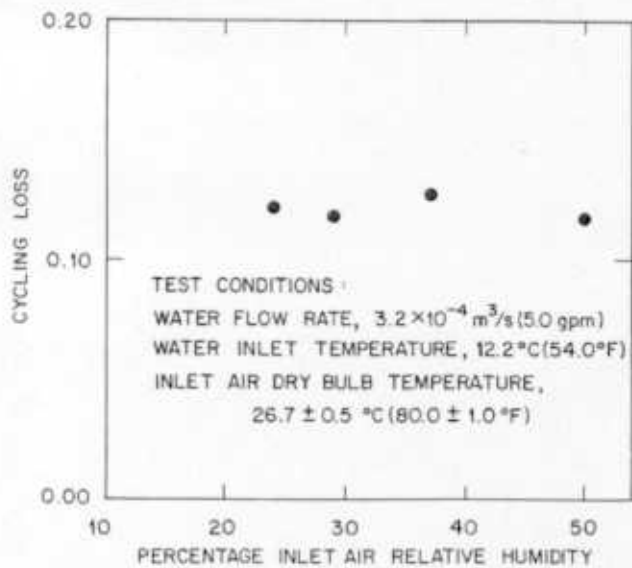


Figure 9. Cooling mode cycling loss versus inlet air relative humidity

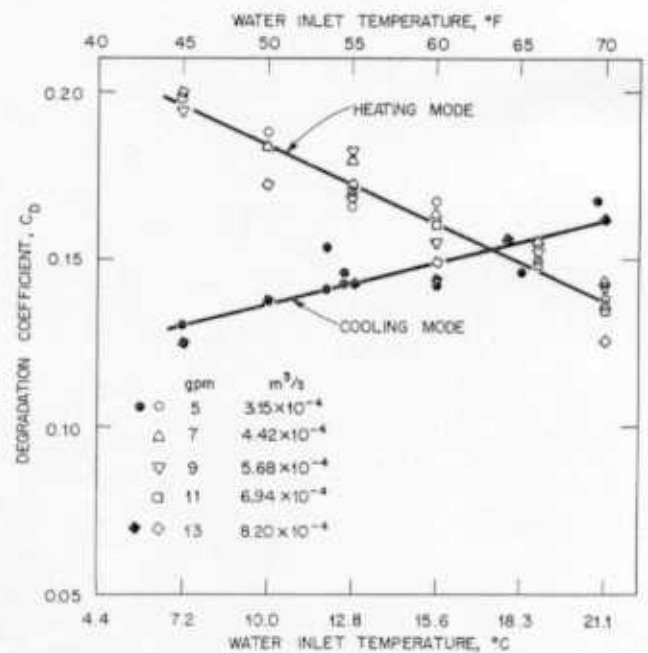


Figure 10. Degradation coefficients versus water inlet temperature

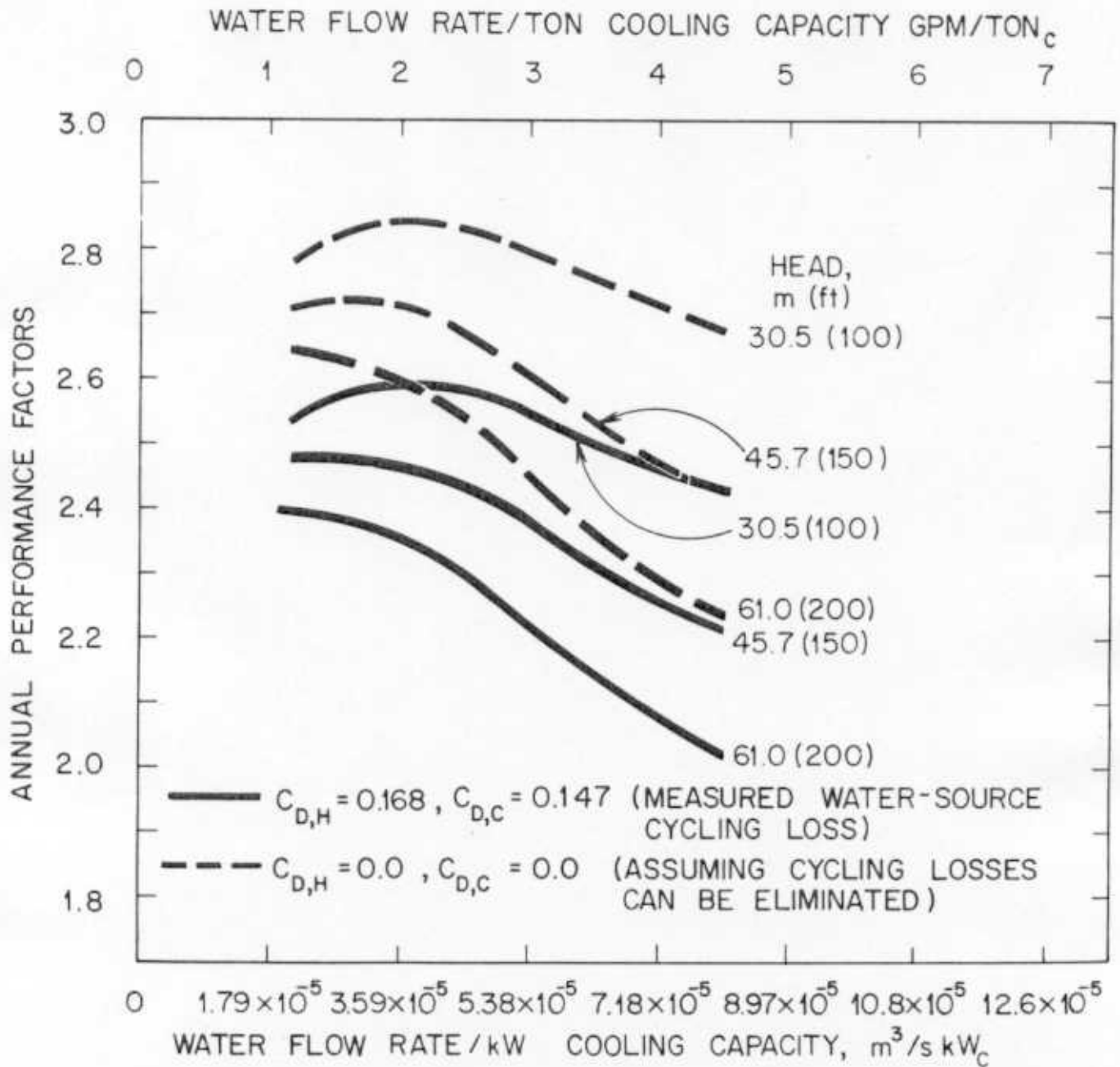


Figure 11. Annual performance factor versus water flow rate per ton of cooling